Optical parametric generation of a mid-infrared continuum in orientation-patterned GaAs

P. S. Kuo, K. L. Vodopyanov, and M. M. Fejer
E. L. Ginzton Laboratory, Stanford University, Stanford, California 94305

D. M. Simanovskii
Hansen Experimental Physics Laboratory, Stanford University, Stanford, California 94305

X. Yu and J. S. Harris
Solid State Photonics Laboratory, Stanford University, Stanford, California 94305

D. Bliss and D. Weyburne
U.S. Air Force Research Laboratory, Hanscom Air Force Base, Massachusetts 01731

Received July 1, 2005; revised manuscript received August 25, 2005; accepted August 26, 2005

We have generated an ultrabroad mid-infrared continuum by using single-pass optical parametric generation (OPG) in orientation-patterned GaAs (OP-GaAs). The spectrum spans more than an octave, from 4.5 to 10.7 μm, measured 20 dB down from the peak. The 17.5 mm long, 0.5 mm thick, all-epitaxially-grown OP-GaAs sample with a 166.6-μm quasi-phase-matching period was pumped with 3.1–3.3 μm wavelength, 1 ps pulses up to 2 μJ in energy. The OPG threshold was observed at 55 nJ pump energy with the pump polarized along the [111] crystal direction. The slope efficiency near threshold was 51%, and the external conversion efficiency was as high as 15%. © 2006 Optical Society of America

OCIS codes: 190.2620, 190.4410, 190.4400, 190.5970.

Gallium arsenide is a promising material for parametric frequency conversion because of its large nonlinear susceptibility (d_{14}=94 pm/V for frequency doubling of λ_f=4 μm),[1] broad infrared transparency range (λ=0.9–17 μm), and high thermal conductivity. Also of interest are its highly symmetric nonlinear susceptibility tensor and linear optical isotropy, which facilitate nonlinear optical interactions that use a rich variety of polarization configurations. However, the optical isotropy of GaAs prevents birefringent phase matching; efficient interactions can instead be obtained by quasi-phase-matching.

Orientation-patterned GaAs (OP-GaAs) is a type of quasi-phase-matched (QPM) GaAs in which periodic inversions of the crystallographic orientation are grown into the material. The advantage of OP-GaAs compared with other QPM GaAs methods [such as diffusion-bonded GaAs (Ref. 2) and Fresnel QPM GaAs (Ref. 3)] is that OP-GaAs has lithographically defined periods, which permit excellent periodicity control and access to small QPM periods. To fabricate OP-GaAs, a process based on photolithography and molecular beam epitaxy is used to grow a thin-film template with periodic crystal inversions.[4,5] A thick film (0.5–1 mm) is then grown upon this template by hydride vapor phase epitaxy to produce bulk OP-GaAs.[6,7] With OP-GaAs, efficient second-harmonic generation,[1] difference-frequency generation,[8] and an optical parametric oscillator tunable from 2 to 11 μm (Refs. 9 and 10) have been demonstrated. In this Letter we describe optical parametric generation (OPG) in OP-GaAs that has resulted in an ultrabroad mid-infrared output spectrum spanning 4.5–10.7 μm.

Anomalously wide tuning bandwidths for parametric processes are associated with wavelength λ_0, where the group-velocity dispersion, $d^2k/d\omega^2$, of a material goes to zero.[11] If one pumps a nonlinear crystal at $\lambda_0/2$, broadband gain around the degenerate signal–idler wavelength can be obtained. Use of OPG is a convenient way to investigate the broadband gain that occurs for GaAs when pumping at $\sim\lambda_0/2$=3.31 μm. Slightly detuning the pump from $\lambda_0/2$ and choosing an appropriate QPM period to compensate for the phase-mismatch results in even broader gain bandwidths (at the expense of some gain variation), as plotted in Fig. 1. Low-intensity gain spectra, proportional to $\mathrm{sinc}^2(\Delta kL/2)$, spanning

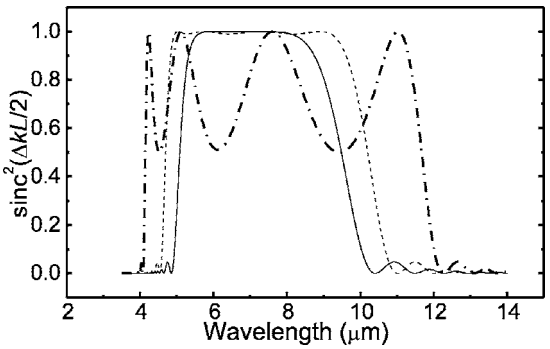

Fig. 1. Normalized gain spectra in the low-gain limit, $\mathrm{sinc}^2(\Delta kL/2)$ (with L=10 mm), for 3.310 μm pump, 173.7 μm period (solid curve); 3.217 μm pump, 166.6 μm period (dashed curve); and 3.059 μm pump, 154.2 μm period (dashed–dotted curve). The last two curves show 1% and 50% gain variation, respectively. These cases all fall within the main, dark band in Fig. 2.

0146-9592/06/010071-3/$0.00

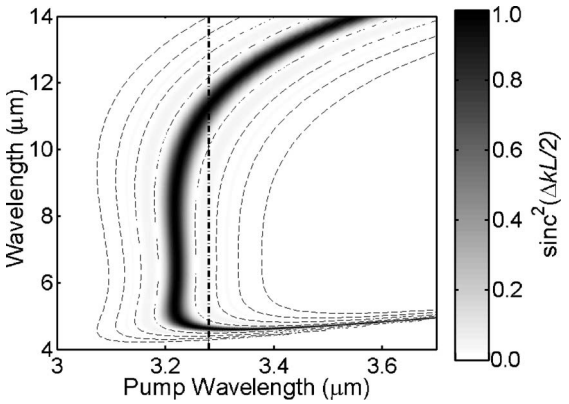

Fig. 2. Gray-scale plot of $\mathrm{sinc}^2(\Delta kL/2)$ for a 166.6 μm QPM period, 10 mm long OP-GaAs sample. Dashed contour curves indicate nodes where $|\Delta kL/2| = m\pi$, $m = 1, 2, 3, 4$.

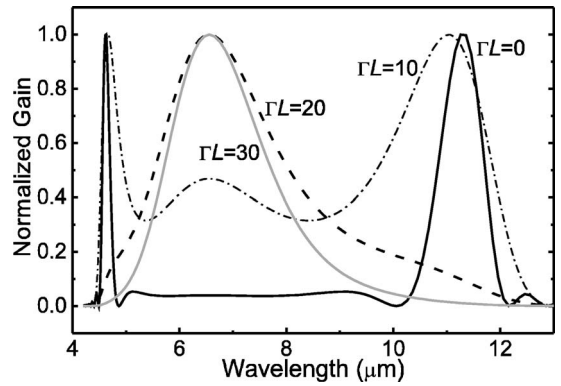

Fig. 3. Theoretical gain spectra for a 3.28 μm pumped, 166.6 μm period OP-GaAs sample for four values of ΓL. At the degenerate point ($\lambda = 6.6$ μm) for an $L = 10$ mm sample, $|\Delta kL/2| \approx 5$. This case is represented by the bold dashed–dotted line in Fig. 2.

well over an octave can be obtained by use of OP-GaAs.

At high intensities, gain bandwidths are further increased through parametric gain broadening.[12] The gain G in a three-frequency process is given by[13]

$$G = \Gamma^2 L^2 \frac{\sinh^2(gL)}{(gL)^2}, \tag{1}$$

where

$$g = [\Gamma^2 - (\Delta k/2)^2]^{1/2}, \tag{2}$$

$$\Gamma^2 = \frac{2\omega_s \omega_i |d_{\mathrm{eff}}|^2 I_p}{n_s n_i n_p \epsilon_0 c^3}. \tag{3}$$

$\Delta k = k_p - k_s - k_i - K_{QPM}$ is the the k-vector mismatch; s, i, and p denote signal, idler, and pump, respectively. The magnitude of the $\Delta k/2$ term in Eq. (2) can be estimated from Fig. 2, which maps $\mathrm{sinc}^2(\Delta kL/2)$ for a 166.6 μm period, 10 mm long OP-GaAs sample. If we take the OPG threshold condition as $G > 10^{10}$, then $\Gamma L > 12.2$, so $\Gamma L > |\Delta kL/2|$ over a broad range of OPG output wavelengths. Figure 3 illustrates an extreme case in which the gain is peaked at degeneracy for high pump intensities but is peaked at well-separated signal–idler wavelengths for low pump intensities. When ΓL is large, the gain spectrum is peaked where Γ is maximized (which occurs at degeneracy because $\Gamma \sim \omega_s \omega_i$ is biggest when $\omega_s = \omega_i$, assuming that $\omega_s + \omega_i = \omega_p$ is fixed), whereas at low gain, the spectrum is peaked only where $\Delta k = 0$ (at widely separated wavelengths). We note that Eqs. (1)–(3) describe mixing for the idealized case of an undepleted, plane-wave pump, but they are useful for qualitative understanding of parametric gain broadening in more general cases.

In our experiment, pump pulses were produced with a Spectra-Physics OPA-800 system. The system used a regeneratively amplified Ti:sapphire laser down-converted through optical parametric amplification and difference-frequency generation to produce 3.1–3.3 μm wavelength, 1 ps duration pulses up to 2 μJ in energy. The OP-GaAs sample was 17.5 mm long and 0.5 mm thick and had a 166.6 μm period. The crystal length was twice the group-velocity-walk-off length between pump and signal waves, so the stationary analysis used above is only approximately correct. The pump was focused to a 75 μm $1/e^2$ intensity radius spot (confocal focusing for the degenerate OPG wavelength near 6.5 μm). The pump and output waves propagated along the [110] crystallographic axis with the pump linearly polarized along the [111] direction such that $d_{\mathrm{eff}} = (2/\pi)(2/\sqrt{3})d_{14}$.[9] The sample was antireflection coated with $R < 0.5\%$ in the signal band, $R < 5\%$ in the idler band, and modest reflectivity at the pump wavelength ($R = 14\%$). The OPG output was characterized with a grating monochromator purged with nitrogen.

Figure 4 shows the OPG output as function of incident pump energy for a 3.25 μm pump wavelength. The OPG threshold was observed at 55 nJ of pump, which is consistent with our calculations based on the $G > 10^{10}$ criterion. The peak intensity at threshold was 0.6 GW/cm^2 (0.6 mJ/cm^2 fluence), which is well below the damage threshold for GaAs. Near OPG threshold, the slope efficiency was 51%, but the curve soon rolls off as pump depletion, and parasitic effects such as sum-frequency generation (SFG) and nonlinear phase shifts become significant. The maximum external conversion efficiency observed was 15% at 140 nJ of pump.

The OPG spectrum for 3.28 μm pump wavelength at 1.4 μJ incident energy is plotted in Fig. 4. The pump wavelength is not at optimum phase-matching

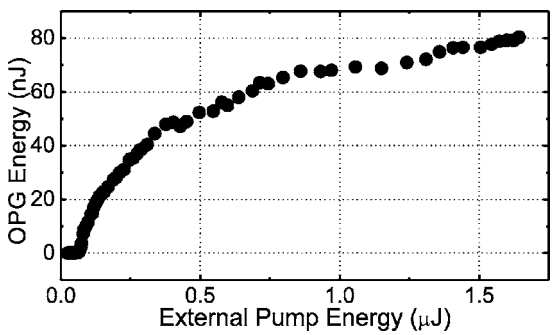

Fig. 4. Total OPG energy as a function of incident pump energy. Threshold was observed at 55 nJ.

for the 166.6 μm period grating, yet we observe a broad output spectrum owing to parametric gain broadening. At 20 dB down from the peak, the spectrum spans 4.5–10.7 μm, well over an octave wide. The spectrum is actually broader than the detection range for our HgCdTe detector, which is limited to $\lambda < 11$ μm.

We believe that some dips in the output spectrum result from phase-matched sum-frequency mixing of portions of the OPG spectrum with the strong pump. In particular, the SFG process, 3.28 μm + 5 μm $\rightarrow$ 1.98 μm, is accidentally third-order quasi-phase-matched by the 166.6 μm period grating. This process depletes the OPG signal near 5 μm, which also reduces the gain at the corresponding idler wavelength at 9.5 μm and accounts for the dips labeled *a* and *b* in Fig. 5. The expected SFG wave at 1.98 μm was directly observed with the monochromator. Origins of other dips in the OPG spectrum are less clear. It is interesting to note that the OPG spectrum remains broad when the pump is tuned to different wavelengths but that the fine structure of the spectrum (i.e., the position and number of the dips) changes in ways that cannot be explained by parasitic SFG only.

There are other nonlinear effects, such as self-phase modulation and self-focusing, that become significant at the large pump intensities used in this experiment. Using the Z-scan technique,[14] we measured the nonlinear refractive index for GaAs at 3.25 μm to be $n_2 = 1.5 \times 10^{-13}$ cm^2/W. At OPG threshold, the maximum nonlinear phase shift caused by the pump pulses is $\Delta\phi_{NL} = (2\pi L/\lambda) n_2 I = 3$. Nonlinear-phase-shift effects become important when $\Delta\phi_{NL} \approx 1$,[15] so it is clear that self-phase modulation and self-focusing are significant under the conditions investigated here. We have observed both spatial distortion and spectral broadening of the transmitted pump. Note that broad bandwidths can be obtained without these high intensities for near-phase-matched cases, such as those shown in Fig. 1.

We characterized the divergence of the OPG by measuring the energy transmitted through an aperture as a function of distance, using a spectrally flat pyroelectric detector. Using this method, we estimate that the divergence angle of the OPG output was approximately twice that of an ideal 6.6 μm wavelength Gaussian beam with the same waist size as the pump.

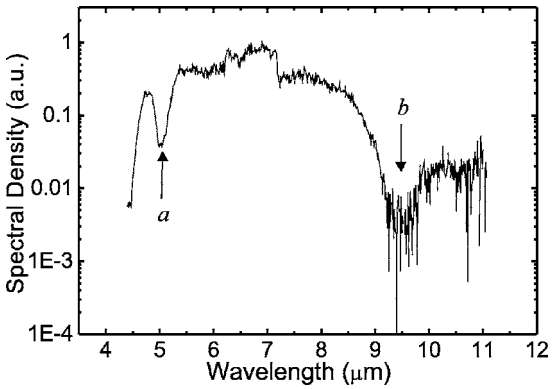

Fig. 5. OPG output spectrum for a 3.28 μm pump at 1.4 μJ energy. Dips at 5 and 9.5 μm (marked *a* and *b*, respectively) are due to parasitic SFG.

This ultrabroad IR spectrum is an interesting ultrafast, near-diffraction-limited "lightbulb" source for various spectroscopic applications for which octave bandwidths combined with tight focusing or a high degree of collimation are required.

This study was supported by the U.S. Air Force Office of Scientific Research under grant F49620-01-1-0428 as well as by BAE Systems under contract RU8444 and Northrup Grumman Corporation under contract 8200044059-4 (the last two under a U.S. Air Force prime contract). P. S. Kuo (pskuo@stanford.edu) acknowledges support from the Lucent graduate research program for women and the Stanford graduate fellowships program.

References

1. T. Skauli, K. L. Vodopyanov, T. J. Pinguet, A. Schober, O. Levi, L. A. Eyres, M. M. Fejer, J. S. Harris, B. Gerard, L. Becouarn, and E. Lallier, Opt. Lett. **27**, 628 (2002).
2. L. Gordon, G. L. Woods, R. C. Eckardt, R. R. Route, R. S. Feigelson, M. M. Fejer, and R. L. Byer, Electron. Lett. **29**, 1942 (1993).
3. R. Haidar, Ph. Kupecek, and E. Rosencher, Appl. Phys. Lett. **83**, 1506 (2003).
4. C. B. Ebert, L. A. Eyres, M. M. Fejer, and J. S. Harris, J. Cryst. Growth **202**, 187 (1999).
5. S. Koh, T. Kondo, M. Ebihara, T. Ishiwada, H. Sawada, H. Ichinose, I. Shoji, and R. Ito, Jpn. J. Appl. Phys., Part 2 **38**, L508 (1999).
6. L. A. Eyres, P. J. Tourreau, T. J. Pinguet, C. B. Ebert, J. S. Harris, M. M. Fejer, L. Becouarn, B. Gerard, and E. Lallier, Appl. Phys. Lett. **79**, 904 (2001).
7. L. A. Eyres, "All-epitaxial orientation-patterned semiconductors for nonlinear optical frequency conversion," Ph.D dissertation (Stanford University, 2001).
8. O. Levi, T. J. Pinguet, T. Skauli, L. A. Eyres, K. R. Parameswaran, J. S. Harris, M. M. Fejer, T. J. Kulp, S. E. Bisson, B. Gerard, E. Lallier, and L. Becouarn, Opt. Lett. **27**, 2091 (2002).
9. K. L. Vodopyanov, O. Levi, P. S. Kuo, T. J. Pinguet, J. S. Harris, M. M. Fejer, B. Gerard, L. Becouarn, and E. Lallier, Opt. Lett. **29**, 1912 (2004).
10. K. L. Vodopyanov, O. Levi, P. S. Kuo, T. J. Pinguet, J. S. Harris, M. M. Fejer, B. Gerard, L. Becouarn, and E. Lallier, in Proc. SPIE **5620**, 63 (2004).
11. A. Birmontas, A. Piskarskas, and A. Stabinis, Sov. J. Quantum Electron. **13**, 1243 (1983).
12. A. J. Campillo, R. C. Hyer, and S. L. Shapiro, Opt. Lett. **4**, 357 (1979).
13. R. L. Byer and R. L. Herbst, in *Nonlinear Infrared Generation*, Y.-R. Shen, ed. (Springer-Verlag, 1977), pp. 81–137.
14. M. Sheik-Bahae, A. A. Said, and E. W. Van Stryland, Opt. Lett. **14**, 955 (1989).
15. G. P. Agrawal, *Nonlinear Fiber Optics*, 3rd ed. (Academic, 2001).